

Monte Carlo Simulation of Inorganic Scintillators Response to Gamma Rays: A Comparative Study

¹N. Ghal-Eh, ²G.R. Etaati and ³M. Mottaghian

¹School of Physics, Damghan University of Basic Sciences, Damghan, Iran

²Department of Physics and Nuclear Science, Amir Kabir University of Technology, Tehran, Iran

³Department of Physics, School of Science, Ferdowsi University of Mashhad, Mashhad, Iran

Abstract: The essential physical processes and the basics of the Monte Carlo simulation of inorganic scintillators response to gamma rays are introduced. The results of two most common used response function generating codes and the corresponding measurements are compared.

PACS: 29.40.Mc

Key words: Inorganic scintillator . Response function . Monte Carlo

INTRODUCTION

Inorganic scintillators are widely used for the detection of ionizing radiations, especially gamma rays, due to their high-Z components. Sodium iodide doped with thallium as an activator, *NaI(Tl)*, is the most widely-used of this type, which shows extremely good light yield, excellent linearity and a quite good detection efficiency [1].

The frequency curve of the number of light photons reached to the photomultiplier tube (PMT) against light (or energy), known as the response function, is an important characteristics of scintillators, which can be obtained either experimentally [2] or by Monte Carlo computations, via the calculation of energy deposited within the detector [3-7] or by applying Monte Carlo code systems such as ETRAN, EGS4, EGS [8], MNCP [9, 10], GEANT4 [11], PETRANS [12], MARTHA [13].

The interaction of gammas with scintillation material, which has to be modelled in order to calculate a reliable response function, includes photoelectric effect, Compton scattering, Rayleigh scattering and pair production. The full energy peak is a result of the photoelectric effect and the full energy absorption through multiple interactions. The incident photon, incoherently scattered by an electron, loses energy and the event appears in the Compton continuum. The single and double escape peaks are due to pair production within the detector and the 511-and 200-keV peaks originate from annihilation radiation and backscattering, respectively. Therefore, different components like Compton edge, Compton background, backscatter peak, escape and annihilation peaks appear in the measured/simulated spectrum.

The processes subsequent to photoelectric absorption are the emission of a fluorescent *X*-ray or an Auger electron. In the photoelectric absorption process, a characteristic *X*-ray is emitted by the absorber atom. In the majority of cases this *X*-ray energy is reabsorbed fairly near the original interaction site. If the photoelectric absorption occurs near a surface of the detector, however, the *X*-ray photon may escape. In this event, the energy deposited in the detector is decreased by an amount equal to the *X*-ray photon energy. Without the *X*-ray escape, the original gamma ray would have been fully absorbed and the resulting pulse would have contributed to the photopeak. With escape, a new category of events is created in which an amount of energy equal to the original gamma ray energy minus the characteristic *X*-ray energy is repeatedly deposited in the detector. Therefore, a new peak will appear in the response function and will be located at a distance equal to the energy of the characteristic *X*-ray below the photopeak. These peaks are generally labelled “*X*-ray escape peaks” and tend to be most prominent at low incident gamma ray energies and for detectors whose surface-to-volume ratio is large [1].

There are several papers devoted to the Monte Carlo modeling of the *NaI* response functions by considering the above processes.

“The use of random numbers in order to model a phenomenon, instrument, etc., which may be of probabilistic nature (*e.g.*, photon interactions with matter) or may not (*e.g.*, integration)” is known as Monte Carlo simulation [14], which is being used in various disciplines [15-18].

Basically, in all Monte Carlo response function generating codes, after defining the source position and detector geometry and related details, the gamma

photons are transported to the sensitive volume of the *NaI* scintillator. Using a random number generator, e.g., RAN3 as in Numerical Recipes [19], the interaction type (photoelectric absorption, Compton scattering, etc.) is determined according to the photon energy and correspondingly, the cross-section [20]. At each step, the energy deposited within the detector and gamma photon trajectories are simulated.

In some Monte Carlo codes (e.g., GEANT4), the scintillation light photons are also transported until it reaches the photocathode of PMT, whilst, some prefer not to include the light transport, therefore as soon as the light is produced, the simulation process is terminated (e.g., EGS4)

In this paper, the structures of two Monte Carlo codes, EGS4 and GEANT4, are introduced in Section 2. The comparison between the results of these two codes and associated experimental data are presented in Section 3. Section 4 concludes the paper and discusses some comparisons among the above two codes.

EGS4 AND GEANT4 MONTE CARLO CODES

EGS4: The EGS4 code system is a well-structured and thoroughly documented system of programs which allow the user to simulate the transport of electrons and photons, with energies above a few keV up to several TeV, in any material [21-23]. It is used to design accelerators and detectors for nuclear and high-energy physics. It has also several applications of medical radiation physics [24-28].

Essentially the User Writes:

1. A user code which handles input, output and the initialization of various parameters.
2. A subroutine to specify the geometry of the particular problem.
3. A scoring routine which keeps the track of the quantities of interest (in this case the energy deposited in the active detector volume).

The EGS4 code system is written in a structured language called Mortran3 [29] developed at Stanford Linear Accelerator Centre (SLAC). It is essentially an extension of standard FORTRAN. Although it is possible to program EGS4 entirely in FORTRAN, the use of Mortran3 results in very much shorter and more readable code.

EGS4 Accounts for the Following Processes:

- Photoelectric effect.
- Compton scattering.
- Bremsstrahlung production
- Positron annihilation in flight and at rest
- Moliere multiple scattering (i.e., Coulomb scattering from nuclei)

- Mueller (e^-e^-) and Bhabha (e^+e^-) scattering
- Continuous energy loss applied to charged particle tracks between discrete interactions. The total stopping power consists of soft bremsstrahlung and collision loss terms. The collision loss itself determined by the (restricted) Bethe-Bloch stopping power with Sternheimer treatment of the density effect
- Pair production
- Coherent (Rayleigh) scattering

The photoelectric effect (and the subsequent X-ray emissions) and Compton scattering which have more significant contributions in shaping the response function of *NaI* scintillator exposed to low-energy photons are discussed in the following subsections.

Photoelectric effect: Every photoelectric absorption is supposed to be caused by iodine, because the absorption probability by iodine is much higher than the probability by sodium. It is assumed that a photon with less than the *K*-shell binding energy is absorbed by removing the *L*-shell electron and that a photon with more than the *K*-shell binding energy can cause both *K*-shell and *L*-shell absorption. Though photoelectric absorption by the outer shells is possible, the occurrence probability is extremely low. The ratio of *K*-shell absorption to the total photoelectric absorption is almost constant, but increases a little as a function of photon energy [30]. Here, the ratio is assumed to be constant at 0.89. When a *K*-shell vacancy is filled by an electron coming from the outer shells, a *K* X-ray or an Auger electron is emitted. The probability of *K* X-ray emission subsequent to *K*-shell absorption ω_K , was obtained from the following equation [30]:

$$\left(\frac{\omega_K}{1-\omega_K}\right)^{1/4} = -A + BZ - CZ^3$$

where *Z* is the atomic number. Using the following $A = 6.4 \times 10^{-2}$, $B = 3.4 \times 10^{-2}$, $C = 1.03 \times 10^{-6}$, ω_K was calculated to be 0.86.

In transitions of electrons coming from the higher shells to the *K*-shell, the important ones are expressed in the Siegbahn notation as follows:

$$K_{\alpha 1} = K - L_{III}, K_{\alpha 2} = K - L_{II}, K_{\beta 1} = K - M_{III},$$

$$K_{\beta 2} = K - N_{III}, K_{\beta 3} = K - M_{II}, K_{\beta 4} = K - N_{II}$$

These transitions were classified into four groups of:

$$K_{\alpha 1}, K_{\alpha 2}, K_{\beta 1} (= K_{\beta 1} + K_{\beta 3} + K_{\beta 2}),$$

$$K_{\beta 2} (= K_{\beta 2} + K_{\beta 4} + \text{other transitions}).$$

Table 1: Probability of transition from outer shells to K-shells and the energy liberated

Shell	Electron Binding energy (keV)	Transition probability from K-shell	Representative K X-ray energy (keV)
K	33.17		
L _{III}	4.56	1.000	28.61
L _{II}	4.85	0.515	28.32
M _{III}	0.88		
M _{II}	0.93	0.273	32.30
M _{IV}	0.63		
N _{III}	0.12	0.057	33.05
N _{II}	0.12		

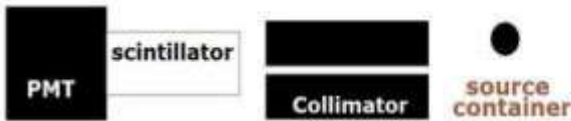


Fig. 1: The experimental setup (Gamma source and NaI scintillation detector)

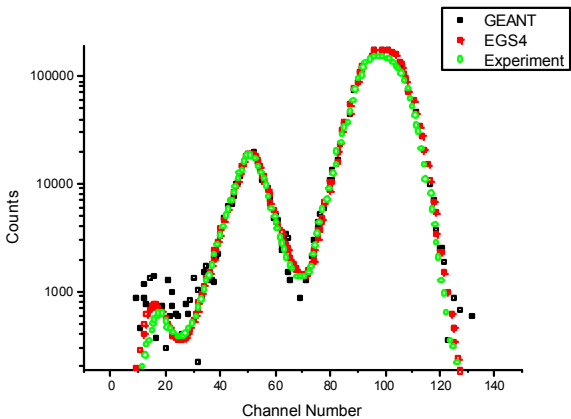


Fig. 2: EGS4, GEANT and experimental response functions of a 2inch by 2inch NaI(Tl) response to 60 keV Am-241 gammas (Peaks from left to right: Compton edge, escape peak, absorbed peak)

Table 1 shows the occurrence probability of each transitions and the energy liberated [27].

For K_{β_1} and K_{β_2} transitions, the emitted X-ray energy is assumed to be constant across their respective emission. X-rays from L-shell absorption and any Auger electrons are assumed to lose all their energy soon after they are generated. A K X-ray is assumed to be emitted in a random direction and is traced until it degenerates under 10 keV of cut-off energy.

Compton scattering: Direction and energy of a photon after Compton scattering are randomly sampled by

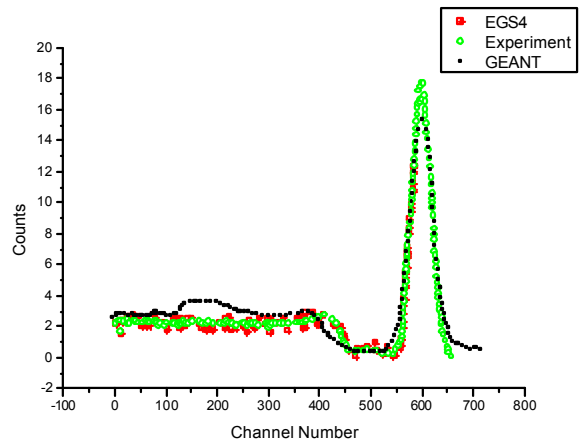


Fig. 3: Comparison of GEANT4 and EGS-simulated data versus experimental spectra for 662 keV photons from Cs-137 gamma source

making use of the Klein-Nishina formula. At low energy, the scattering angle distribution of a photon differs from the Klein-Nishina law, since the binding between an electron and a nucleus perturbs the scattering. Nevertheless, the photoelectric effect occurs so frequently that the perturbation is expected to make little change in calculation. Here, the Compton scattering features are decided in accordance with the Klein-Nishina formula.

A simple source-detector geometry shown in Fig. 1 was considered and the EGS4 (without the contribution of surrounding materials) and GEANT (with the contribution of surrounding materials) simulation results compared with the corresponding measurements have been illustrated in Fig. 2.

The comparison in Fig. 2 shows an overall good agreement at higher pulse heights (less than 3% maximum discrepancy), whilst the discrepancy has increased at Compton edge, which is supposed to be due to an approximate contributions of surrounding materials inclusion to GEANT.

GEANT4: GEANT, or *GEometry ANd Tracking* code, is an object-oriented toolkit for simulating the passage of particles through matter. The physics processes it provides (hadronic, electromagnetic and optical) cover a comprehensive set of particles and materials over a wide range of energy. Besides the physics, it also offers a complete set of functionality, like tracking, visualization and geometry description. It has been developed by a large worldwide collaboration and created exploiting a rigorous software engineering and object-oriented approach. The Geant4 kit, which can be publicly downloaded from the web, includes the C++ source code, an extensive documentation and several tutorial examples, showing complete applications of Geant 4 to realistic experimental set-ups. The toolkit can

be installed on several supported platforms (Linux, SUN and Windows) [11].

All aspects of the simulation process have been included in the toolkit:

- Geometry of the system
- Materials involved
- Fundamental particles of interest
- Generation of primary events
- Tracking of particles through materials and electromagnetic fields
- Physics processes governing particle interactions
- Response of sensitive detector components
- Generation of event data
- Storage of events and tracks
- Visualization of the detector and particle trajectories
- Capture and analysis of simulation data at different levels of detail and refinement

Users may construct stand-alone applications or applications built upon another object-oriented framework. In either case the toolkit will support them from the initial problem definition to the production of results and graphics for publication. To this end, the toolkit includes:

- User interfaces,
- Built-in steering routines and
- Command interpreters

which operate at every level of the simulation.

For the purpose of this study, GEANT4 was run to simulate the dominant photon interaction with the matter, occurring in the energy range from 10 keV to 100 GeV. Therefore, the self-absorption and scattering of photons within the sample and all possible interaction of the photons with the detector housing as well as with the *NaI* crystal have been automatically taken into account.

In order to simulate the response function of the *NaI* detector, the precise dimension of the crystal and its position in the detector housing must be entered into the *detector description routine* of the GEANT. In some studies, as the dimensions are not adequately accurate, to achieve a precise simulation, the reported size and position of the crystal are verified by scanning front and side faces of the detector with a narrowly collimated beam of gamma rays coming from a point source [32]. As shown in Fig. 3, GEANT4 and EGS4 simulation vs. experimental data show an overall good agreement (less than 5% discrepancy) with experimental data, except at low energies, whose source of discrepancy is being investigated.

CONCLUSIONS

Inorganic scintillators have been widely used since their discovery by Hofstadter. Their response to gamma-rays is important especially for the online elemental analysis, medical imaging application, position-sensitive detection, etc. During recent years, a large amount of experimental and calculational work has focused on studying the response function of this type of scintillators (especially *NaI(Tl)*). The paper presents a review on the capabilities of GEANT4 and EGS4 in simulating the scintillator response function, followed by corresponding experimental results. For the case of simple geometry like the one presented in this paper, both GEANT and EGS4 can produce reliable simulation results.

REFERENCES

1. Knoll, G.F., 1989. Radiation Detection and Measurement, Wiley, New York.
2. Heath, R.L., 1964. Scintillation spectrometry, gamma-ray spectrum catalogue. USAEC Report IDO-16880, USA.
3. Berger, M.J. and J. Doggett, 1956. Response function of thallium-activated sodium-iodide scintillation counters. J. Res. NBS, 56: 355-366.
4. Hubbell, J.H., 1958. Response of a large sodium-iodide detector to high-energy X-rays. Rev. Sci. Instrum., 29: 65-68.
5. Zerby, C.D. and H.S. Moran, 1962. Calculation of the pulse-height response of NaI(Tl) scintillation counters. Nucl. Instrum. Meth., A 14: 115-124.
6. Berger, M.J. and S.M. Seltzer, 1972. Response functions for sodium iodide scintillation detectors. Nucl. Instrum. Meth., 104: 317-332.
7. Nakamura, T., 1972. Monte Carlo calculation of efficiencies and response functions of NaI (Tl) crystals for thick disk gamma-ray sources and its application to Ge (Li) detectors. Nucl. Instrum. Meth., 105: 77-89.
8. Jenkins, T.M., W.R. Nelson and A. Rindi, 1988. Monte Carlo Transport of Electrons and Photons. Plenum Press, New York, pp: 221-246, 307-321.
9. Briesmeister, J.F., 1997. MCNP-a general Monte Carlo N-particle transport code. Los Alamos National Laboratory Report, LA-12625-M.
10. Arthur Forster, R. *et al.*, 2004. MCNP™ Version 5, Nucl. Instrum. Meth., B213: 82-86.
11. Agostinelli, S. *et al.*, 2003. GEANT4-a simulation toolkit, Nucl. Instrum. Meth., A506: 250-303.
12. Hu-Xia Shi, Bo-Xian Chen, Ti-Zhu Li and Di Yun, 2002. Precise Monte Carlo simulation of gamma-ray response functions for an NaI (Tl) detector. Appl. Rad. and Isot., 57: 517-524.

13. Saito, K. and S. Moriuchi, 1981. Monte Carlo calculation of accurate response functions for a NaI (Tl) detector for gamma rays. Nucl. Instrum. Meth., 185: 299-308.
14. Ghal-Eh, N., 2003. Modelling light transport in scintillators. Ph.D Thesis, Ferdowsi University of Mashhad, Mashhad, Iran.
15. Peiravi, A., 2008. Estimation of expected lifetime and reliability during burn in and field operation using Markov chain Monte Carlo simulations. World Applied Sciences Journal, 4: 748-754.
16. Vajpai, J. and J.B. Arun, 2009. Chaotic nature of energy demand. World Applied Sciences Journal, 7: 834-845.
17. Gandomi, A.H., M.G. Sahab, A. Rahaei and M. Safari Gorji, 2008. Development in mode shape-based structural fault identification technique. World Applied Sciences Journal, 5: 29-38.
18. Niknam, T., B. Bahmani Firouzi and M. Nayeripour, 2008. An efficient hybrid evolutionary algorithm for cluster analysis. World Applied Sciences Journal, 4: 300-307.
19. Press, W.H., W.T. Vetterling, S.A. Teukolsky and B.P. Flannery, 1999. Numerical recipes in Fortran 77: The art of Scientific Computing, Cambridge University Press.
20. Ahmadzadeh, E., 2001. Monte Carlo simulation of NaI (Tl) response to gamma rays. M.Sc. Thesis, Physics Department, School of Science, Ferdowsi University of Mashhad, Mashhad, Iran.
21. Ford, R.L. and W.R. Nelson, The EGS4 code system: Computer programs for the Monte Carlo simulation of electromagnetic cascade showers. Stanford Linear Accelerator Centre Report SLAC-210.
22. Nelson, W.R., H. Hirayama, D.W. Rogers, The EGS4 Code System. Stanford Linear Accelerator Centre, Report SLAC-265.
23. Nelson, W.R. and D.W. Rogers, 1988. Structure and operation of the EGS4 code system. In: Jenkins, T.M., W.R. Nelson, A. Rindi (Eds.). Monte Carlo Transport of Electrons and Photons, Plenum, New York, pp: 287-310.
24. Kilic, A., 1995. A theoretical and experimental investigation of polarized X-rays for the *in vivo* measurements of heavy metals. Ph.D. Thesis, University of Wales (Swansea), UK.
25. Lewis, D.G., A. Kilic and C.A. Ogg, 1955. Adaptation of the EGS4 Monte Carlo code for the design of a polarized source for X-ray fluorescence analysis of platinum and other heavy metals *in vivo*. In: Predecki, P.K. *et al.*, Editors, Advances in X-ray Analysis, Plenum, New York, 38: 579-583.
26. Jeraj, R., P.J. Keall and P.M. Ostwald, 1999. Comparisons between MCNP, EGS4 and experiment for clinical electron beams. Phys. Med. Biol., 44: 705-717.
27. Siebers, J.V., P.J. Keall, B. Libby, R. Mohan, 1999. Comparison of EGS4 and MCNP4b Monte Carlo codes for generation of photon phase space distributions for a Varian 2100C. Phys. Med. Biol., 44: 3009-3026.
28. Zaidi, H., Relevance of accurate Monte Carlo modeling in nuclear medical imaging. Med. Phys., 26: 574-608.
29. Nelson, W.R., H. Hirayama and D.W. Rogers, 1985. The EGS4 Code System. Stanford Linear Accelerator Centre, Report SLAC-265.
30. Siegbahn, K., 1965. Alpha-, Beta-and Gamma-Ray Spectroscopy, North-Holland, Amsterdam.
31. Wapstra, A.H., G.J. Nijgh and R. Van Lieshout, 1959. Nuclear Spectroscopy Tables, North-Holland, Amsterdam.
32. Ashrafi, S., S. Anvarian and S. Sobhanian, 2006. Monte-Carlo modeling of a NaI (Tl) Scintillator. J. Radioanal. Nucl. Chem., 269: 95-98.